

Optimization of Metabolic Oligosaccharide Engineering with Ac_4GalNAk and Ac_4GlcNAk by an Engineered Pyrophosphorylase

Anna Cioce,^{*} Ganka Bineva-Todd,^{*} Anthony J. Agbay, Junwon Choi, Thomas M. Wood, Marjoke F. Debets, William M. Browne, Holly L. Douglas, Chloe Roustan, Omur Y. Tastan, Svend Kjaer, Jacob T. Bush, Carolyn R. Bertozzi, and Benjamin Schumann^{*}



Cite This: *ACS Chem. Biol.* 2021, 16, 1961–1967



Read Online

ACCESS |



Metrics & More

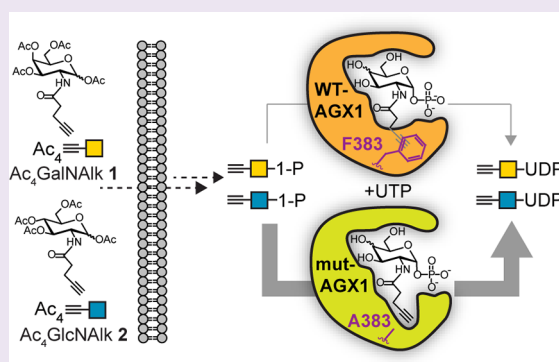


Article Recommendations



Supporting Information

ABSTRACT: Metabolic oligosaccharide engineering (MOE) has fundamentally contributed to our understanding of protein glycosylation. Efficient MOE reagents are activated into nucleotide-sugars by cellular biosynthetic machineries, introduced into glycoproteins and traceable by bioorthogonal chemistry. Despite their widespread use, the metabolic fate of many MOE reagents is only beginning to be mapped. While metabolic interconnectivity can affect probe specificity, poor uptake by biosynthetic salvage pathways may impact probe sensitivity and trigger side reactions. Here, we use metabolic engineering to turn the weak alkyne-tagged MOE reagents Ac_4GalNAk and Ac_4GlcNAk into efficient chemical tools to probe protein glycosylation. We find that bypassing a metabolic bottleneck with an engineered version of the pyrophosphorylase AGX1 boosts nucleotide-sugar biosynthesis and increases bioorthogonal cell surface labeling by up to two orders of magnitude. A comparison with known azide-tagged MOE reagents reveals major differences in glycoprotein labeling, substantially expanding the toolbox of chemical glycobiology.



INTRODUCTION

Protein glycosylation is an essential modulator of biological processes. Chemical MOE reagents have developed into important alternatives to protein-based binding reagents to profile the roles of glycans in cellular processes.^{1–4} Monosaccharides with chemical modifications can be fed to living cells as hydrophobic caged analogues that cross the plasma membrane. Once deprotected by (thio)esterases, these monosaccharides are metabolically activated and introduced into the glycome by the activity of glycosyltransferases (GTs).^{1,4–6} Modifications such as azides or alkynes can be probed by bioorthogonal ligation using Cu(I)-catalyzed azide–alkyne cycloaddition (CuAAC) to allow for the visualization and characterization of glycoconjugates.^{2,4,7,8} While it is generally accepted that small chemical perturbations are compatible with metabolic activation, the actual fate and turnover efficiency of modified monosaccharides is only beginning to be understood. The key to being used by GTs is the biosynthesis of modified nucleotide-sugars, such as derivatives of uracil diphosphate (UDP)-activated *N*-acetylglactosamine (GalNAc) and *N*-acetylglucosamine (GlcNAc) (Figure 1A). The biosynthetic salvage pathway of GalNAc derivatives features the kinase GALK2 and the pyrophosphorylases AGX1/2, while GlcNAc derivatives have to be activated by the kinase NAGK, the mutase AGM, as well as AGX1/2.^{9,10} In the cytosol of mammalian cells, the derivatives of UDP-

GalNAc and UDP-GlcNAc can be interconverted by the UDP-GalNAc/GlcNAc 4'-epimerase GALE, which interconnects both nucleotide-sugar pools. Epimerization substantially decreases the glycan specificity while enhancing the labeling efficiency of certain MOE reagents and can be suppressed by careful choice of the chemical modification.^{10–12} Once biosynthesized, the derivatives of UDP-GalNAc and UDP-GlcNAc can be used as substrates by cellular GTs, including the large polypeptide GalNAc transferase (GalNAc-T) family in the secretory pathway and a myriad of GlcNAc transferases in several cellular compartments.

Recent years have seen increasing evaluation of the metabolic fate of MOE reagents. Although the enzymes of GalNAc and GlcNAc salvage pathways generally display reduced efficiency toward modifications on the acetamide side chain, the relatively small azide group is accepted as part of reliable MOE reagents.^{10,12–15} In contrast, bulkier modifications prevent the enzymatic activation of GalNAc and GlcNAc analogues.^{11,16,17} Yu et al. thus developed an

Special Issue: Chemical Glycobiology

Received: January 18, 2021

Accepted: March 29, 2021

Published: April 9, 2021



ACS Publications

© 2021 The Authors. Published by
American Chemical Society

1961

<https://doi.org/10.1021/acschembio.1c00034>
ACS Chem. Biol. 2021, 16, 1961–1967

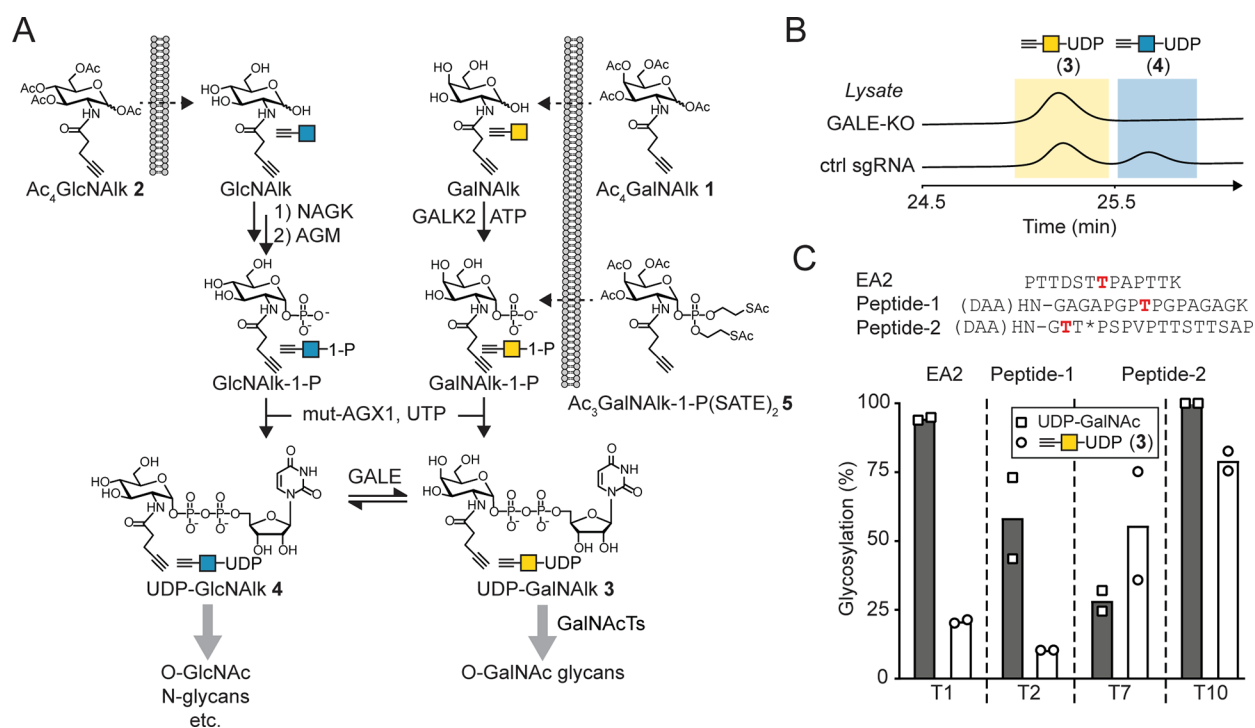


Figure 1. Metabolic fate of GalNAk and GlcNAk. (A) Biosynthesis of UDP-GalNAk 3 and UDP-GlcNAk 4 from caged precursors using salvage pathways. Dashed arrows indicate diffusion across membranes and (thio)-esterases. (B) *In vitro* epimerization of UDP-GalNAk 3 (yellow) to UDP-GlcNAk 4 (blue) using a GALE-containing (ctrl sgRNA) cell lysate or a GALE-KO lysate as a control, as assessed by high-performance anion exchange chromatography (HPAEC). The reaction was also performed using purified GALE, and the retention times were compared to those of the standards (Figure S1). (C) *In vitro* glycosylation with purified GalNAc-Ts of synthetic peptides using UDP-GalNAk 3 or UDP-GalNAc as substrates. The amino acids in red are new glycosylation sites. T* denotes α -D-GalNAc-Thr. Data are individual measurements of independent duplicates and means. The reactions using UDP-GalNAc as a substrate have been used previously.¹¹

engineered version of AGX1 (mutant F383G) to increase substrate promiscuity and biosynthesize UDP-GlcNAc analogues from the corresponding GlcNAc-1-phosphate analogues that can be delivered through caged precursors.¹⁶ We have used the similar F383A mutant, herein termed mut-AGX1, to biosynthesize UDP-GalNAc analogues that would not normally be made in the living cell.^{4,11,17} Somewhat surprisingly and contrary to azide-tagged analogues of similar size, Batt et al. found that, after feeding the commercial MOE reagents Ac₄GalNAk 1 and Ac₄GlcNAk 2, the most simple alkyne-tagged UDP-GalNAc and UDP-GlcNAc derivatives, UDP-GalNAk 3 and UDP-GlcNAk 4, are biosynthesized in varying and often low efficiency in mammalian cells (Figure 1A).¹⁸ Previous experience by us and Yu et al. on delivering UDP-sugar analogues with even longer side chains suggested that AGX1-mediated pyrophosphorylation may be a roadblock to the biosynthesis of UDP-GalNAc/GlcNAc derivatives.^{16,17} These longer derivatives could only be delivered through caged sugar-1-phosphates that are of limited stability and tedious to synthesize. We thus sought to investigate if simply enhancing pyrophosphorylation with mut-AGX1 would allow delivery from the readily available reagents Ac₄GalNAk 1 and Ac₄GlcNAk 2.

Here, we profile the metabolic fate of the weak MOE reagents Ac₄GalNAk 1 and Ac₄GlcNAk 2 in order to turn both reagents into highly efficient tools to probe cell surface glycosylation. We find that mut-AGX1 effectively biosynthesizes UDP-GalNAk 3 and UDP-GlcNAk 4 with greatly increased efficiency over WT-AGX1 from caged precursors that can thus be used to profile cell surface protein

glycosylation. By suppressing GALE-mediated epimerization, we further find that UDP-GalNAk 3 and UDP-GlcNAk 4 are used to glycosylate non-identical glycoprotein subsets to azide-tagged analogues, potentially due to differential acceptance by GTs. We show that close monitoring of the biosynthetic fate enables the development of highly effective MOE reagents.

RESULTS AND DISCUSSION

To study the metabolic fate of UDP-GalNAk 3 and UDP-GlcNAk 4, we first assessed *in vitro* whether both reagents are epimerized by GALE (Figure 1B). The incubation of synthetic 3 with either a wild type (WT) GALE-containing lysate of control cells transfected with a non-targeting single guide (sg) RNA,¹⁷ or purified GALE led to epimerization to 4, as detected either by ion-pair high-performance liquid chromatography (HPLC) or high-performance anion exchange chromatography (HPAEC). A lysate of GALE-KO cells did not lead to epimerization.¹⁷ We next profiled the suitability of UDP-GalNAk 3 as a substrate for members of the GalNAc-T family. GalNAc-Ts prime highly abundant mucin-type protein O-GalNAc glycans, and the acceptance of 3 would thus correlate with high cell surface labeling efficiency. Synthetic peptides served as acceptor substrates in *in vitro* glycosylation experiments. Compared to the native substrate UDP-GalNAc, UDP-GalNAk 3 was used with a lower but well-measurable efficiency by GalNAc-T1 and T2 and a similar efficiency by GalNAc-T7 and T10 (Figure 1C). The isoenzymes T7 and T10 differ from T1 and T2 in their preference of pre-O-GalNAc-glycosylated substrate peptides, which may hint to the

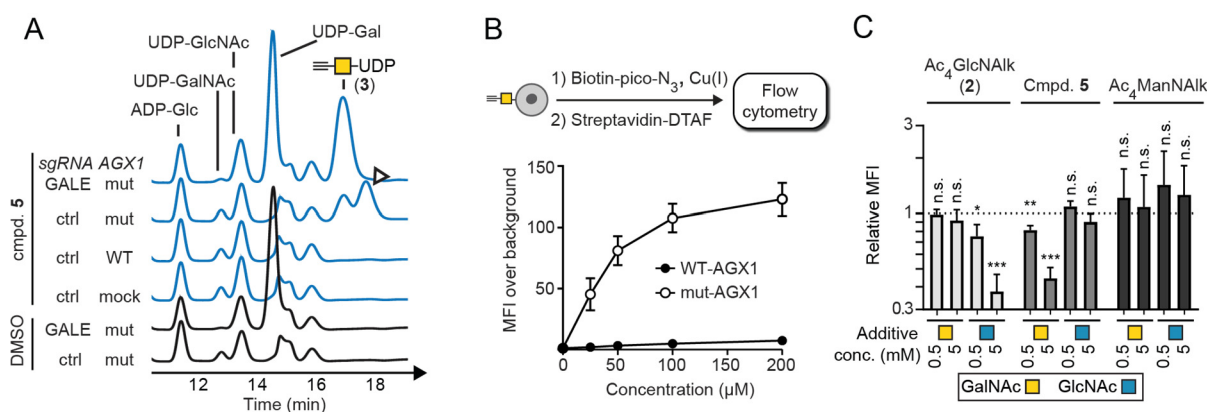


Figure 2. Mut-AGX1-mediated biosynthesis of UDP-GalNAk 3 and cell surface labeling. (A) Metabolite profiling of K-562 cells based on AGX1 expression (mock signifies empty vector) and the presence of GALE by HPAEC. The arrowhead depicts the epimerization of UDP-GalNAk 3 to UDP-GlcNAk 4. ADP-glucose was added as an external standard. Data are representative of two independent experiments. (B) Dose response of cell surface labeling of AGX1-stably transfected K-562 cells after feeding 3 as assessed by flow cytometry. Data are mean \pm SEM as fold increase from DMSO-treated cells from at least three independent experiments. Error bars for WT-AGX1 data are too small to be shown. (C) Competition assay of cell surface labeling in mut-AGX1-transfected GALE-KO K-562 cells fed with 50 μ M caged GalNAk-1-phosphate 5, 50 μ M Ac₄GlcNAk 2, or 10 μ M Ac₄ManNAk by different concentrations of GalNAc or GlcNAc. Data are means \pm SD from three independent experiments. Statistical significance was assessed by unpaired, two-tailed *t* test against labeling experiments without additives (dashed line). Asterisks indicate *P* values: **P* < 0.05; ***P* < 0.01; ****P* < 0.001. n.s. nonsignificant. DTAF = dichlorotriazinylamino fluorescein; MFI = median fluorescence intensity.

use of UDP-GalNAk 3 as a GalNAc-T subset-selective substrate.²⁰

We next studied the biosynthesis of UDP-GalNAk 3 and UDP-GlcNAk 4 in cells fed with caged, membrane-permeable precursors. Since AGX1 has been identified as a metabolic bottleneck of other modified GalNAc analogues, we synthesized caged GalNAk-1-phosphate 5 to specifically probe the AGX1-mediated biosynthesis of UDP-GalNAk 3.^{4,11,17} We tested UDP-sugar biosynthesis from 5 in K-562 cells with either normal GALE expression or a GALE-KO and stably transfected with either mut-AGX1, WT-AGX1, or an empty vector. HPAEC revealed measurable biosynthesis of both UDP-GalNAk 3 and UDP-GlcNAk 4 in the presence of mut-AGX1 but not WT-AGX1 (Figure 2A and Figure S2). The levels of UDP-GalNAk 3 and UDP-GlcNAk 4 were in the same range as the levels of native UDP-GalNAc and UDP-GlcNAc. Free GalNAk-1-phosphate was detectable in all cases, as observed by comparison with a synthetic standard (Figure S2). In the absence of GALE, UDP-GlcNAk was not detectable, indicating that UDP-GalNAk 3 is biosynthesized by mut-AGX1 and subsequently epimerized by GALE in the cytosol.

We then assessed metabolic cell surface labeling mediated by caged GalNAk-1-phosphate 5 by flow cytometry. Clickable biotin-picolyl azide was used in noncytotoxic Cu(I)-click CuAAC conditions followed by streptavidin-DTAF to visualize labeling.^{8,21} The presence of mut-AGX1 led to a dose-dependent increase of fluorescence by up to two orders of magnitude compared to WT-AGX1 (Figure 2B). Of note, the presence of WT-AGX1 still led to low but discernible cell surface labeling, indicating that UDP-GalNAk 3 can be biosynthesized at levels that are too low to detect chromatographically. This was especially pronounced in GALE-KO cells in which no endogenous UDP-GalNAc is present to compete with UDP-GalNAk 3 as a substrate of GalNAc-Ts (Figure 2B and Figure S3B). A labeling difference of one order of magnitude was observed between cells expressing WT-AGX1 and mut-AGX1 when fed with Ac₄GlcNAk 2, indicating that mut-AGX1 also mediates UDP-GlcNAk 4 biosynthesis

(Figure S3A). Increasing the UDP-GalNAc levels in GALE-KO cells by supplementing cell culture media with free GalNAc led to a decrease of an UDP-GalNAk 3-dependent labeling signal (Figure 2C and Figure S3C).¹⁷ Likewise, the labeling signal by Ac₄GlcNAk 2 was abrogated by the addition of free GlcNAc (Figure 2C). In contrast, labeling by the control compound Ac₄ManNAk, a MOE reagent that enters the biosynthetic pathway of the sugar sialic acid, was unchanged irrespective of AGX1 overexpression or the addition of free GalNAc or GlcNAc (Figure 2C and Figure S3B). Enhancing the levels of native UDP-sugars thus competed out the incorporation of GalNAk and GlcNAk, but not ManNAk, into glycoproteins. We concluded that AGX1 is likely a bottleneck in the biosynthesis of both UDP-GalNAk 3 and UDP-GlcNAk 4, impairing metabolic labeling, which can be enhanced by a stable overexpression of mut-AGX1 but not WT-AGX1. Our data further indicate that Ac₄GalNAk 1 exhibits low-level metabolic glycoprotein labeling without mut-AGX1 expression, in line with findings of Zaro et al.⁷ UDP-GalNAk 3 formation is not measurable under these conditions, underlining the highly inefficient biosynthesis of 3 by the GalNAc salvage pathway without mut-AGX1.¹⁸

As the overexpression of mut-AGX1 enabled cell surface labeling from Ac₄GlcNAk 2, GlcNAk-1-phosphate biosynthesis from the free monosaccharide by NAGK/AGM1 was apparently not a major metabolic bottleneck. We next assessed whether UDP-GalNAk 3 biosynthesis followed the same principles, which would, in turn, allow us to use the readily available MOE reagent Ac₄GalNAk 1 instead of caged GalNAk-1-phosphate 5. We found that mut-AGX1, but not WT-AGX1, efficiently biosynthesized UDP-GalNAk 3 and UDP-GlcNAk 4 from the peracetylated precursors Ac₄GalNAk 1 and Ac₄GlcNAk 2, respectively, in living cells (Figure S4). We note that the “upstream” precursors Ac₄GalNAk 1 and Ac₄GlcNAk 2 required longer feeding times (12–16 h instead of 6–9 h) than caged GalNAk-1-phosphate 5 for UDP-sugar biosynthesis to be detected, in line with additional enzymatic reactions being required. At these

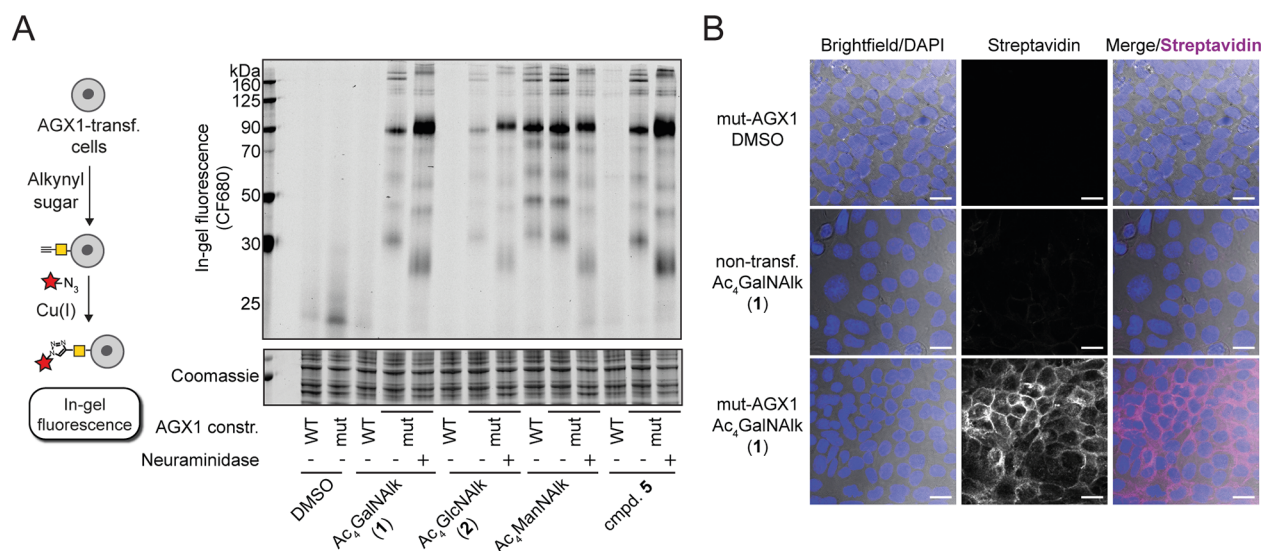


Figure 3. Mut-AGX1 enables efficient metabolic labeling with caged precursors of GalNAc and GlcNAc. (A) Cell surface labeling of AGX1-transfected K-562 cells fed with 50 μM Ac₄GalNAk 1, 50 μM Ac₄GlcNAk 2, 10 μM Ac₄ManNAk, or 25 μM caged GalNAk-1-phosphate 5 as assessed by on-cell CuAAC with the NIR fluorophore CF680-picolyl azide and in-gel fluorescence. Cells were treated with the neuraminidase SialEXO before the click reaction where indicated. Data are representative of two independent experiments. (B) Fluorescence microscopy of mut-AGX1-expressing or nontransfected 4T1 cells fed with DMSO or 25 μM Ac₄GalNAk 1 treated with biotin-picolyl-azide under on-cell CuAAC conditions and visualized with streptavidin-AF647. Data are representative of two independent experiments. Scale bar: 20 μm .

time points, free GalNAk-1-phosphate is clearly detectable (Figure S4). These data indicated that WT-AGX1-mediated pyrophosphorylation is likely the rate-determining step in the biosynthesis of UDP-GalNAk 3 and UDP-GlcNAk 4. The expression of mut-AGX1 likely renders the upstream activation steps NAGK/AGM and GALK2 as rate-determining.

We next visualized the impact of metabolic engineering on glycoprotein labeling by Ac₄GalNAk 1 and Ac₄GlcNAk 2. Following the feeding of AGX1-transfected K-562 cells with alkyne-containing monosaccharide precursors, cell surfaces were either treated with a neuraminidase that removes sialic acid from glycoproteins, or left untreated. The living cells were then subjected to CuAAC with the clickable near-infrared fluorophore CF680-picolyl azide, and labeled cell surface glycoproteins were analyzed by in-gel fluorescence.¹⁷ Under these conditions, the compounds Ac₄GalNAk 1, Ac₄GlcNAk 2, and caged GalNAk-1-phosphate 5 exhibited mut-AGX1-dependent labeling while the control reagent Ac₄ManNAk labeled glycoproteins irrespective of the AGX1 construct used (Figure 3A). Neuraminidase treatment led to an increase of signals in all cases except for Ac₄ManNAk-labeled cells, consistent with an increased availability of GalNAc- and GlcNAc-carrying alkyne tags toward click reagents when the layer of sialic acid was enzymatically trimmed.^{11,17} While these results suggest that neither GlcNAk nor GalNAk enter the sialic acid pool through metabolic interconversion, more detailed experiments are needed to exclude such a metabolic crosstalk.¹² Of note, the dependence on mut-AGX1 for GalNAk/GlcNAk labeling emphasizes that UDP-sugar formation is a prerequisite for efficient labeling, excluding previously reported nonenzymatic cysteine adduct formation that typically happens under very high concentrations of peracetylated sugars.^{22,23} We next visualized glycocalyx labeling by fluorescence microscopy. We chose adherent murine 4T1 cells to allow for straightforward imaging and further demonstrated the robustness of our approach. Clickable biotin picolyl azide and streptavidin-AF647 readily detected a large

enhancement of Ac₄GalNAk 1-mediated cell surface labeling in 4T1 cells stably expressing mut-AGX1 compared to nontransfected cells (Figure 3B). In contrast, cell surface labeling by the AGX1-independent MOE reagent Ac₄ManNAk remained unchanged upon mut-AGX1 transfection (Figure S5).

Due to the GALE-mediated interconversion of UDP-GalNAk 3 and UDP-GlcNAk 4, the glycoprotein profiles labeled by both MOE reagents Ac₄GalNAk 1 and Ac₄GlcNAk 2 were identical (Figure 3A). To assess the contribution of each UDP-sugar to the signal, we profiled the glycoprotein patterns in GALE-KO cells that functionally separate UDP-GalNAk 3 and UDP-GlcNAk 4 (Figure 4A). Cells were grown in GalNAc-containing media to maintain the native levels of metabolites such as UDP-GalNAc, allowing for comparison with GALE-expressing control cells when all cell lines were transfected with mut-AGX1. DMSO feeding did not lead to discernible labeling (Figure 4A, lanes 1 and 2).

While GALE-expressing control cells displayed identical labeling patterns when fed with either Ac₄GalNAk 1 or Ac₄GlcNAk 2 (Figure 4A, lanes 3 and 4), GALE-KO had a striking effect on labeling patterns. In GALE-KO cells, Ac₄GalNAk 1 contributed highly intense glycoprotein bands at approximately 100 and 40 kDa (Figure 4A, lane 5), while Ac₄GlcNAk 2 contributed a diffuse pattern of lower overall intensity (Figure 4A, lane 6). These results suggested that separating the UDP-GalNAk 3 and UDP-GlcNAk 4 pools led to labeling of different subsets of glycoproteins. In contrast, feeding Ac₄ManNAk led to similar band patterns in both GALE-expressing and GALE-KO cell lines (Figure 4A, lanes 7 and 8), indicating that sialylation is not affected by GALE-KO. We speculated that the intense bands labeled by UDP-GalNAk 3 (Figure 4A, lanes 3–5) are highly GalNAc-glycosylated mucin-domain-containing glycoproteins. To test this notion, we treated cagedGalNAk-1-phosphate 5-fed, mut-AGX1-expressing K-562 cells with CF680-picolyl-azide under CuAAC conditions to fluorescently tag the GalNAk-

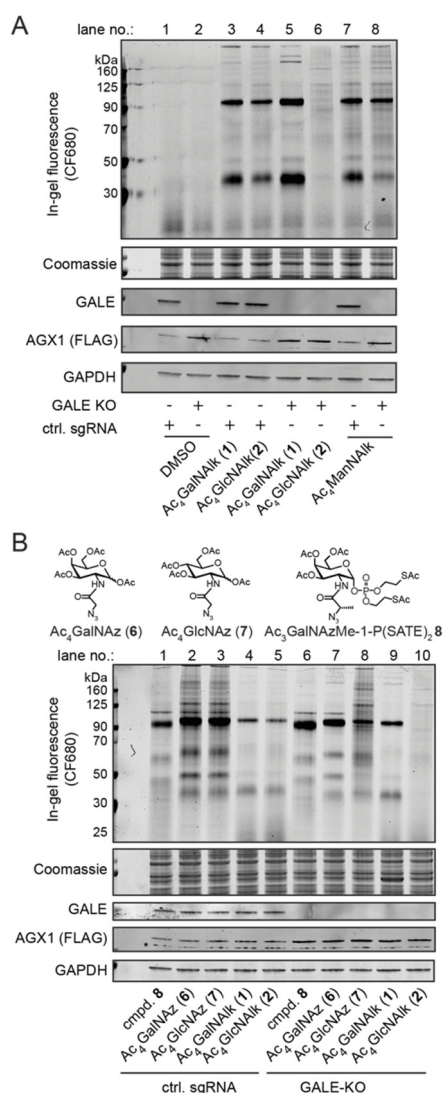


Figure 4. GalNAIk- and GlcNAIk-mediated labeling of glycoprotein subsets. (A) Cell surface labeling of mut-AGX1-transfected K-562 GALE-KO or control sgRNA-expressing cells fed with 10 μ M Ac₄GalNAik 1, 50 μ M Ac₄GlcNAik 2, or 10 μ M Ac₄ManNAik as assessed by on-cell CuAAC and in-gel fluorescence. Data are representative of two independent experiments. (B) Comparison of cell surface labeling of mut-AGX1-transfected K-562 GALE-KO or control sgRNA-expressing cells fed with 10 μ M Ac₄GalNAik 1, 50 μ M Ac₄GlcNAik 2, 3 μ M Ac₄GalNAz 6, 8 μ M Ac₄GlcNAz 7, or 100 μ M caged GalNAzMe-1-phosphate 8. Data are representative of two independent experiments.

containing glycoproteome. We then subjected the living cells to different concentrations of the mucin protease StcE or the more promiscuous *O*-glycoprotease OpeRATOR (Figure S6).²⁴ Treatment with both proteases led to a decrease of cell surface glycoprotein signal in a dose-dependent manner, while a signal was recovered as fluorescently-labeled broad bands of lower molecular weight in the supernatant. Several glycoprotein bands were digested by OpeRATOR, but not StcE, indicating that labeling of nonmucins containing *O*-GalNAc glycans was observed. These data confirm that GalNAik enters mucin-domain-containing proteins and other *O*-GalNAc-glycosylated proteins.

We next compared the Ac₄GalNAik 1 and Ac₄GlcNAik 2 labeling band patterns in GALE-KO or control cells with

previously characterized, azide-containing MOE reagents Ac₄GalNAz 6 and Ac₄GlcNAz 7 (Figure 4B). Both reagents are converted to azide-tagged UDP-GlcNAc/GalNAc analogues that are interconvertible by GALE.^{10–12} We further used the *O*-GalNAc-specific reagent Ac₃GalNAzMe-1-P-(SATE)₂ 8, a precursor to an epimerization-resistant, azide-tagged UDP-GalNAc analogue that is not a substrate for GALE in the living cell.¹¹ To ensure that band patterns are comparable between azide- and alkyne-tagged monosaccharides, we used the same NIR-fluorophore CF680 with either alkyne or picolyl azide groups for CuAAC. Compound 8 showed a band pattern attributable to *O*-GalNAc glycosylation in GALE-containing and GALE-KO cells (Figure 4B, lanes 1 and 6). Ac₄GalNAz 6/Ac₄GlcNAz 7 (Figure 4B, lanes 2 and 3) labeled the same band pattern in GALE-containing cells, consistent with the interconversion of azide-tagged UDP-sugar pools.^{10,11} This labeling pattern was somewhat different from the pattern observed after feeding GALE-containing cells Ac₄GalNAik 1/Ac₄GlcNAik 2 (Figure 4B, lanes 4 and 5), with more bands being visible with azide-tagged monosaccharide analogues. These findings can be explained by UDP-GalNAz being a better substrate for the commonly expressed glycosyltransferases GalNAc-T1 and T2 than UDP-GalNAik 3 (Figure 1C).^{11,19} Upon GALE-KO, Ac₄GalNAz 6 and Ac₄GlcNAz 7 led to different band patterns, as reported before (Figure 4B, lanes 7 and 8).¹¹ In comparison, the Ac₄GalNAik 1-labeled band pattern in GALE-KO cells resembled only a subset of the pattern seen from Ac₄GalNAz 6 or compound 8 feeding (Figure 4B, lane 9), indicating that UDP-GalNAik 3 labels a subset of *O*-GalNAc glycoproteins. Finally, Ac₄GlcNAik 2 exhibited a diffuse labeling pattern in GALE-KO cells (Figure 4B, lane 10) similar to that of the azide-tagged counterpart Ac₄GalNAz 7. Taken together, these data suggest that UDP-GalNAik 3 and UDP-GlcNAik 4 label different sets of glycoproteins but are interconnected by GALE in the living cell. Structurally simple azide- and alkyne-tagged GalNAc/GlcNAc derivatives label particular glycoprotein subsets and should thus serve as orthogonal but potentially complementary MOE reagents in the presence of mut-AGX1. Western blot analysis with an antibody against AGX1 indicated that our expression constructs lead to an approximately 2–3-fold overexpression, suggesting that metabolic engineering does not require abundant expression levels of mut-AGX1 (Figure S7).

We have shown that comprehensive metabolic profiling can turn weak MOE reagents into efficient chemical biology tools to profile cellular glycosylation. The expression of mut-AGX1 enhances labeling by Ac₄GalNAik 1 and Ac₄GlcNAik 2 by orders of magnitude, substantially expanding the toolbox for glycobiology. While our approach relies on cell transfection, the plasmids we used are based on transposase-mediated stable integration, which is compatible even with hard-to-transfect cell lines and more complex model systems such as organoids.¹¹ Our work focused on improving metabolic labeling efficiency with Ac₄GalNAik 1/Ac₄GlcNAik 2. While we showed that the corresponding activated sugars UDP-GalNAik 3/UDP-GlcNAik 4 can be incorporated in GalNAc- and GlcNAc-containing glycoconjugates, we did not assess their fine specificity for certain subtypes of glycans. We and others have previously focused on assessing such specificity for similar MOE reagents,^{11,25} and further studies extending this work are underway.

■ ASSOCIATED CONTENT

SI Supporting Information

The Supporting Information is available free of charge at <https://pubs.acs.org/doi/10.1021/acscchembio.1c00034>.

Figures of *in vitro* epimerization, metabolite profiling, dose response of cell surface labeling, fluorescence microscopy, in-gel fluorescence, Western blot analysis, ^1H and ^{13}C NMR spectra and discussions of experimental and characterization details (PDF)

Primary data and plasmids are available upon request. Compounds are available upon request as long as stocks last.

■ AUTHOR INFORMATION

Corresponding Author

Benjamin Schumann – Department of Chemistry, Imperial College London, W12 0BZ London, United Kingdom; The Chemical Glycobiology Laboratory, The Francis Crick Institute, NW1 1AT London, United Kingdom; orcid.org/0000-0001-5504-0147; Email: b.schumann@imperial.ac.uk

Authors

Anna Cioce – Department of Chemistry, Imperial College London, W12 0BZ London, United Kingdom; The Chemical Glycobiology Laboratory, The Francis Crick Institute, NW1 1AT London, United Kingdom

Ganka Bineva-Todd – The Chemical Glycobiology Laboratory, The Francis Crick Institute, NW1 1AT London, United Kingdom

Anthony J. Agbay – Department of Chemistry, Stanford University, Stanford, California 94305, United States; orcid.org/0000-0003-0466-5977

Junwon Choi – Department of Chemistry, Stanford University, Stanford, California 94305, United States; orcid.org/0000-0001-6004-5524

Thomas M. Wood – Department of Chemistry, Stanford University, Stanford, California 94305, United States

Marjoke F. Debets – Department of Chemistry, Stanford University, Stanford, California 94305, United States; orcid.org/0000-0002-5176-0072

William M. Browne – Department of Chemistry, Imperial College London, W12 0BZ London, United Kingdom; The Chemical Glycobiology Laboratory, The Francis Crick Institute, NW1 1AT London, United Kingdom

Holly L. Douglas – Mycobacterial Metabolism and Antibiotic Research Laboratory, The Francis Crick Institute, NW1 1AT London, United Kingdom

Chloe Roustan – Structural Biology Science Technology Platform, The Francis Crick Institute, NW1 1AT London, United Kingdom

Omur Y. Tastan – The Chemical Glycobiology Laboratory, The Francis Crick Institute, NW1 1AT London, United Kingdom

Svend Kjaer – Structural Biology Science Technology Platform, The Francis Crick Institute, NW1 1AT London, United Kingdom

Jacob T. Bush – GlaxoSmithKline, Stevenage, Hertfordshire SG1 2NY, United Kingdom; orcid.org/0000-0001-7165-0092

Carolyn R. Bertozzi – Department of Chemistry, Stanford University, Stanford, California 94305, United States;

Howard Hughes Medical Institute, Stanford, California 94305, United States; orcid.org/0000-0003-4482-2754

Complete contact information is available at: <https://pubs.acs.org/doi/10.1021/acscchembio.1c00034>

Author Contributions

[☆]A.C. and G.B.-T. contributed equally. A.C., M.F.D., J.T.B., C.R.B., and B.S. conceived the project and planned experiments. A.C., G.B.-T., A.J.A. H.L.D., and B.S. performed experiments. J.C., T.M.W., W.M.B., C.R., and S.K. made and contributed key reagents. A.C., G. B.-T., A.J.A., M.F.D., and B.S. analyzed data. A.C., G.B.-T., and B.S. wrote the paper with input from all authors.

Funding

The authors are thankful for generous funding by Stanford University, Stanford Chemistry, Engineering and Medicine for Human Health (ChEM-H), and Howard Hughes Medical Institute. This work was supported by NIH Grant R01 CA200423 (to C.R.B.) and by the Francis Crick Institute (A.C., G.B.-T., and B.S.), which receives its core funding from Cancer Research UK Grant FC001749, UK Medical Research Council Grant FC001749, and Wellcome Trust Grant FC001749. M.F.D. was supported by a Dutch Research Council (NWO) Rubicon Postdoctoral Fellowship. W.M.B. was supported by a PhD studentship funded by Engineering and Physical Sciences Research Council (EPSRC) Centre for Doctoral Training in Chemical Biology – Innovation for the Life Sciences Grant EP/S023518/1 and GlaxoSmithKline. H.L.D. acknowledges funds from Wellcome Trust New Investigator Award 104785/B/14/Z. A.J.A. was supported by a Stanford ChEM-H undergraduate scholarship. This research was funded in whole, or in part, by the Wellcome Trust [FC001749 and 104785/B/14/Z]. For the purpose of Open Access, the author has applied a CC BY public copyright license to any Author Accepted Manuscript version arising from this submission.

Notes

The authors declare no competing financial interest.

■ ACKNOWLEDGMENTS

The authors would like to thank D. Fox for help with HPAEC experiments, K. Pedram for providing StcE, M. Pratt for helpful discussions, P. Walker for advice on vector choice, and A. Garza-Garcia for helpful discussions on HPLC. The authors would like to thank R. D'Antuono of the Crick Advanced Light Microscopy STP for support and assistance in this work. The authors are grateful for support by the Francis Crick Institute Cell Services and Peptide Chemistry Science Technology Platforms.

■ REFERENCES

- (1) Sletten, E. M., and Bertozzi, C. R. (2009) Bioorthogonal Chemistry: Fishing for Selectivity in a Sea of Functionality. *Angew. Chem., Int. Ed.* 48 (38), 6974–6998.
- (2) Parker, C. G., and Pratt, M. R. (2020) Click Chemistry in Proteomic Investigations. *Cell* 180 (4), 605–632.
- (3) Zol-Hanlon, M. I., and Schumann, B. (2020) Open Questions in Chemical Glycobiology. *Commun. Chem.* 3 (1), 1–5.
- (4) Cioce, A., Malaker, S. A., and Schumann, B. (2021) Generating Orthogonal Glycosyltransferase and Nucleotide Sugar Pairs as Next-Generation Glycobiology Tools. *Curr. Opin. Chem. Biol.* 60, 66–78.

- (5) Mahal, L. K., Yarema, K. J., and Bertozzi, C. R. (1997) Engineering Chemical Reactivity on Cell Surfaces through Oligosaccharide Biosynthesis. *Science* 276 (5315), 1125–1128.
- (6) Hang, H. C., Yu, C., Pratt, M. R., and Bertozzi, C. R. (2004) Probing Glycosyltransferase Activities with the Staudinger Ligation. *J. Am. Chem. Soc.* 126 (1), 6–7.
- (7) Zaro, B. W., Yang, Y. Y., Hang, H. C., and Pratt, M. R. (2011) Chemical Reporters for Fluorescent Detection and Identification of O-GlcNAc-Modified Proteins Reveal Glycosylation of the Ubiquitin Ligase NEDD4–1. *Proc. Natl. Acad. Sci. U. S. A.* 108 (20), 8146–8151.
- (8) Besanceney-Webler, C., Jiang, H., Zheng, T., Feng, L., Soriano Del Amo, D., Wang, W., Klivansky, L. M., Marlow, F. L., Liu, Y., and Wu, P. (2011) Increasing the Efficacy of Bioorthogonal Click Reactions for Bioconjugation: A Comparative Study. *Angew. Chem., Int. Ed.* 50 (35), 8051–8056.
- (9) Peneff, C., Ferrari, P., Charrier, V., Taburet, Y., Monnier, C., Zamboni, V., Winter, J., Harnois, M., Fassy, F., and Bourne, Y. (2001) Crystal Structures of Two Human Pyrophosphorylase Isoforms in Complexes with UDPGlc(Gal)NAc: Role of the Alternatively Spliced Insert in the Enzyme Oligomeric Assembly and Active Site Architecture. *EMBO J.* 20 (22), 6191–6202.
- (10) Boyce, M., Carrico, I. S., Ganguli, A. S., Yu, S. H., Hangauer, M. J., Hubbard, S. C., Kohler, J. J., and Bertozzi, C. R. (2011) Metabolic Cross-Talk Allows Labeling of O-Linked β -N-Acetylglucosamine-Modified Proteins via the N-Acetylgalactosamine Salvage Pathway. *Proc. Natl. Acad. Sci. U. S. A.* 108 (8), 3141–3146.
- (11) Debets, M. F., Tastan, O. Y., Wisnovsky, S. P., Malaker, S. A., Angelis, N., Moeckl, L. K. R., Choi, J., Flynn, H., Wagner, L. J. S., Bineva-Todd, G., Antonopoulos, A., Cioce, A., Browne, W. M., Li, Z., Briggs, D. C., Douglas, H. L., Hess, G. T., Agbay, A. J., Roustan, C., Kjaer, S., Haslam, S. M., Snijders, A. P., Bassik, M. C., Moerner, W. E., Li, V. S. W., Bertozzi, C. R., and Schumann, B. (2020) Metabolic Precision Labeling Enables Selective Probing of O-Linked N-Acetylgalactosamine Glycosylation. *Proc. Natl. Acad. Sci. U. S. A.* 117 (41), 25293–25301.
- (12) Shajahan, A., Supekar, N. T., Wu, H., Wands, A. M., Bhat, G., Kalimurthy, A., Matsubara, M., Ranzinger, R., Kohler, J. J., and Azadi, P. (2020) Mass Spectrometric Method for the Unambiguous Profiling of Cellular Dynamic Glycosylation. *ACS Chem. Biol.* 15 (10), 2692–2701.
- (13) Hang, H. C., Yu, C., Kato, D. L., and Bertozzi, C. R. (2003) A Metabolic Labeling Approach toward Proteomic Analysis of Mucin-Type O-Linked Glycosylation. *Proc. Natl. Acad. Sci. U. S. A.* 100 (25), 14846–14851.
- (14) Woo, C. M., Iavarone, A. T., Spiciari, D. R., Palaniappan, K. K., and Bertozzi, C. R. (2015) Isotope-Targeted Glycoproteomics (IsoTaG): A Mass-Independent Platform for Intact N- and O-Glycopeptide Discovery and Analysis. *Nat. Methods* 12 (6), 561–567.
- (15) Pouilly, S., Bourgeaux, V., Piller, F., and Piller, V. (2012) Evaluation of Analogues of GalNAc as Substrates for Enzymes of the Mammalian GalNAc Salvage Pathway. *ACS Chem. Biol.* 7 (4), 753–760.
- (16) Yu, S. H., Boyce, M., Wands, A. M., Bond, M. R., Bertozzi, C. R., and Kohler, J. J. (2012) Metabolic Labeling Enables Selective Photocrosslinking of O-GlcNAc-Modified Proteins to Their Binding Partners. *Proc. Natl. Acad. Sci. U. S. A.* 109 (13), 4834–4839.
- (17) Schumann, B., Malaker, S. A., Wisnovsky, S. P., Debets, M. F., Agbay, A. J., Fernandez, D., Wagner, L. J. S., Lin, L., Li, Z., Choi, J., Fox, D. M., Peh, J., Gray, M. A., Pedram, K., Kohler, J. J., Mrksich, M., and Bertozzi, C. R. (2020) Bump-and-Hole Engineering Identifies Specific Substrates of Glycosyltransferases in Living Cells. *Mol. Cell* 78 (5), 824–834.
- (18) Batt, A. R., Zaro, B. W., Navarro, M. X., and Pratt, M. R. (2017) Metabolic Chemical Reporters of Glycans Exhibit Cell-Type-Selective Metabolism and Glycoprotein Labeling. *ChemBioChem* 18 (13), 1177–1182.
- (19) Choi, J., Wagner, L. J. S., Timmermans, S. B. P. E., Malaker, S. A., Schumann, B., Gray, M. A., Debets, M. F., Takashima, M., Gehring, J., and Bertozzi, C. R. (2019) Engineering Orthogonal Polypeptide GalNAc-Transferase and UDP-Sugar Pairs. *J. Am. Chem. Soc.* 141 (34), 13442–13453.
- (20) de las Rivas, M., Lira-Navarrete, E., Gerken, T. A., and Hurtado-Guerrero, R. (2019) Polypeptide GalNAc-Ts: From Redundancy to Specificity. *Curr. Opin. Struct. Biol.* 56, 87–96.
- (21) Uttamapinant, C., Tangepeerachaikul, A., Grecian, S., Clarke, S., Singh, U., Slade, P., Gee, K. R., and Ting, A. Y. (2012) Fast, Cell-Compatible Click Chemistry with Copper-Chelating Azides for Biomolecular Labeling. *Angew. Chem., Int. Ed.* 51 (24), 5852–5856.
- (22) Qin, W., Qin, K., Fan, X., Peng, L., Hong, W., Zhu, Y., Lv, P., Du, Y., Huang, R., Han, M., Cheng, B., Liu, Y., Zhou, W., Wang, C., and Chen, X. (2018) Artificial Cysteine S-Glycosylation Induced by Per-O-Acetylated Unnatural Monosaccharides during Metabolic Glycan Labeling. *Angew. Chem., Int. Ed.* 57 (7), 1817–1820.
- (23) Qin, K., Zhang, H., Zhao, Z., and Chen, X. (2020) Protein S-Glyco-Modification through an Elimination-Addition Mechanism. *J. Am. Chem. Soc.* 142 (20), 9382–9388.
- (24) Malaker, S. A., Pedram, K., Ferracane, M. J., Bensing, B. A., Krishnan, V., Pett, C., Yu, J., Woods, E. C., Kramer, J. R., Westerlind, U., Dorigo, O., and Bertozzi, C. R. (2019) The Mucin-Selective Protease StcE Enables Molecular and Functional Analysis of Human Cancer-Associated Mucins. *Proc. Natl. Acad. Sci. U. S. A.* 116 (15), 7278–7287.
- (25) Pedowitz, N. J., and Pratt, M. R. (2021) Design and synthesis of metabolic chemical reporters for the visualization and identification of glycoproteins. *RSC Chem. Biol.*, in press.